DOI: 10.1002/ejic.200901165

f,f Homodinuclear and d,f or f,f′ Heterodinuclear Complexes with a [2+2] Macrocyclic Compartmental Schiff Base

Sergio Tamburini,*[a] Valentina Peruzzo,[a] Franco Benetollo,[a] and P. Alessandro Vigato[a]

Keywords: Lanthanides / Schiff bases / Macrocycles / Heteronuclear complexes

The [2+2] compartmental macrocyclic complexes [Ln(H_2-L)(NO_3)], where H_2-L is the cyclic Schiff base, derived from the condensation of 2,6-diformyl-4-chlorophenol (H-L^A) or 2,6-diformyl-4-methylphenol (H-L^B) and *N*,*N*-bis(2-aminoethyl)-2-hydroxybenzylamine·3HCl (HA′·3HCl), contains a free N_3O_3 coordination chamber and can act as a ligand toward an identical or a different lanthanide(III) ion and a d transition metal(II) ion to give the related f,f homodinuclear [Ln_2(L)(X)$_2$] and f,f′ heterodinuclear [LnLn′(L)(X)$_2$] or d,f heterodinuclear [LnM(L)(X)] complexes. They have been characterized by ESEM-EDS, ESI-MS, and IR and ^{1}H and ^{13}C NMR spectroscopy. The X-ray single-crystal analysis of the [2+1] acyclic complex [Lu_2(L′)$_2$], derived from partial hydrolysis of the related [2+2] homodinuclear complex [Lu_2(L)(Cl)$_2$], followed by the loss of one lutetium(III) ion with the free formyl groups turning into diacetal ones, is also reported.

Introduction

The synthesis of macrocyclic Schiff base dinuclear complexes derived from the [2+2] template condensation of 2,6-diformyl-4-substituted phenol and a variety of primary diamines has successfully been experienced for more than three decades.[1–5] This synthetic pathway gives rise to symmetric systems containing two identical adjacent coordination chambers capable of securing two metal ions in close proximity. The shape of these coordination moieties mainly depends on the employed amine.[6,7]

In these studies the coordinating cavity of the two adjacent coordination chambers was progressively enlarged to allow the encapsulation of two larger metal ions [i.e., lanthanide(III) metal ions]. This was achieved by using primary amines of the type $H_2N(CH_2)_nX(CH_2)_nNH_2$ (X = NH, NCH_3, O, S) with longer aliphatic or aromatic chains bearing additional donor atoms.[6,7] Furthermore, these amines were further functionalized by the insertion, especially at the secondary amine group, of appropriate coordinating groups (i.e., phenol, pyridine, carboxylic acid, etc.) to modify the recognition ability of the resulting coordinating chambers towards specific metal ions. Thus, the reaction of sodium 2,6-diformyl-4-X-phenolate (X = -CH_3, -Cl) with *N*,*N*-bis(2-aminoethyl)-2-hydroxybenzylamine, followed by in situ transmetalation with Cd(ClO_4)$_2$ or Mn(ClO_4)$_2$ resulted in the formation of [Cd_2(H_2-L)](ClO_4)$_2$ and [Mn_2(H-L)](ClO_4), respectively, whose structures contain two octahedral metal(II) ions bridged by two μ_2-phenoxy oxygen atoms. Each six-coordinate metal(II) ion resides in a N_3O_3 unit composed of two imino nitrogen atoms, one tertiary nitrogen atom, two phenolic oxygen atoms, as well as one oxygen atom from one of the pending phenolic groups. The phenolic oxygen atom of each pendant arm is bound to the adjacent manganese ion and two pendant groups are on the same side of the macrocycle.[8]

These macrocycles are not stable in the presence of specific metal ions and can lose the -$CH_2C_6H_4OH$ lateral arms, as observed when the above-condensation reaction is carried out in the presence of Fe(ClO_4)$_2$. This reaction affords [Fe(H_2-L′)(Cl)](ClO_4)$_2$, where H_2-L′ is the 21-membered [2+2] asymmetric compartmental Schiff base macrocycle derived from the release of a lateral arm of H_2-L and the subsequent ring contraction of the free chamber by ring closure. In consequence of these reactions, the resulting complex is a mononuclear species with a six-coordinate distorted octahedral iron(III) ion, equatorially surrounded by two phenoxy oxygen atoms, one imine nitrogen atom, and the adjacent secondary amine nitrogen atom and axially bound by the other imine nitrogen and a chloride anion. The free chamber, owing to the presence of a NH group, undergoes ring contraction with the formation of an additional five-membered ring.[8]

In this paper, 2,6-diformyl-4-X-phenol (X = -CH_3, -Cl) and *N*,*N*-bis(2-aminoethyl)-2-hydroxybenzylamine·3HCl were successfully employed in the synthesis of the related [2+2] macrocyclic derivatives, capable of forming, thanks to the coordinating ability of the phenol group appended to the central nitrogen atom of the diamine precursor, stable mononuclear lanthanide(III) complexes that can evolve into f,f homodinuclear and f,f′ or d,f heterodinuclear species whose physicochemical properties were examined by envi-

---

[a] Istituto di Chimica Inorganica e delle Superfici – C.N.R.,
Corso Stati Uniti 4, 35127 Padova, Italy
E-mail: sergio.tamburini@icis.cnr.it

Supporting information for this article is available on the WWW under http://dx.doi.org/10.1002/ejic.200901165.

ronmental scanning electron microscope energy-dispersive X-ray spectroscopy (ESEM-EDS), IR, ^{1}H, and ^{13}C NMR spectroscopy, and ESI-MS data. In the past, the use of similar ligands, without these lateral coordinating functionalities, often resulted in mixtures of complexes in consequence of transmetalation, site migration, and demetalation reactions.[9]

Furthermore, the X-ray diffraction structure of the [2+1] acyclic complex $[Y_2(L')_2]$, resulting from recrystallization of the related [2+2] macrocyclic complex $[Y_2(L)(Cl)_2]\cdot 3.5H_2O$, is also reported. During the crystallization procedure, partial hydrolysis at the imine groups occurred with the formation of the [2+1] acyclic Schiff base $[L']^{3-}$, whose formyl groups turned into the related diacetal derivatives.

These data revealed the need to pay attention to the synthesis and properties of [2+1] acyclic ligands and related complexes, and the results of our efforts are briefly reported.

Results and Discussion

Attention was primarily focused on the synthesis of the [2+1] acyclic ligand and related complexes, as they can represent useful intermediates in the preparation of homo- and heterodinuclear complexes and, hence, in setting up a step-by-step pathway. In this synthetic route, the obtainment of well-characterized acyclic complexes with the metal ion in a defined site occupancy is of great relevance in the subsequent condensation reaction with a second amine precursor and a second metal ion.

Appropriate knowledge of compounds arising from different steps allows the generation of metal complexes with the metal ion in a previously designed site and, in turn, to verify the occurrence of site migration, transmetalation, or demetalation processes.

The acyclic ligand H_3-acy obtained by condensation of H-L^B with HA$'\cdot$3HCl under high dilution conditions in $CHCl_3$ is sparingly soluble in $CHCl_3$ and CH_3CN, thus preventing further condensation and complexation reactions in these solvents. This ligand is soluble in alcohol where, however, acetal or diacetal formation at both carbonyl groups can take place, giving rise to the H_3-L$'$ derivative (Scheme 1).

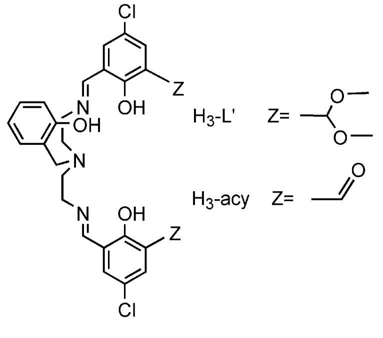

Scheme 1.

The reaction between the preformed acyclic ligand and one equivalent of the desired lanthanide(III) salt in the presence of base in methanolic solution results in the formation of a mixture of products. The IR spectrum of the yttrium(III) complex is characterized by a broad band in the range 1670–1600 cm^{-1} probably due to the sum of the ν(C=O) and ν(C=N) strong absorption bands arising from different species (i.e., carbonyls or acetals), as proved by the occurrence of very complex NMR spectra.

The template reaction of H-L^B, HA$'\cdot$3HCl, $Ln(X)_3\cdot n$-H_2O, and NaOH in a 2:1:1:6 molar ratio in methanol affords, according to elemental analyses, the [2+1] mononuclear acyclic diacetal complex [Ln(L$'$)]. In the IR spectrum there is only a ν(C=N) band at 1630 cm^{-1}, which is typical of the coordinated iminic group. IR and NMR spectroscopy revealed the absence of the C=O groups, which turned in the less reactive acetal groups.

To avoid the formation of acetals and/or a mixture of products, template reactions were carried out in $CHCl_3$/CH_3OH (95:5). However, the addition of a methanol solution of HA$'\cdot$3HCl, NaOH, and YCl_3 to a warm $CHCl_3$ solution of 2,6-diformyl-4-methylphenol again gives rise to an unidentified mixture of products.

In conclusion, attempts to isolate pure [2+1] lanthanide(III) acyclic complexes failed; in any case, a mixture of diformyl and/or diacetal derivatives, not useful for further condensation reaction, occurs.

Synthesis and Characterization of the [2+2] Macrocyclic Complexes

In light of the above-reported results, the [2+2] macrocyclic f,f homodinuclear and f,f$'$ or d,f heterodinuclear complexes have been prepared, according to Scheme 2, through a template or step-by-step procedure by following the different synthetic pathways A–E.

Also, 2,6-diformyl-4-methylphenol was employed as a diformyl precursor in the analogous synthetic procedures reported in Scheme 2. The obtained complexes, thanks to their favorable solubility in organic solvents, revealed to be useful in confirming the results obtained for the compounds derived from the chlorophenol precursor.

The synthesis of the macrocyclic ligand H_4-L (Scheme 3) by addition of HA$'\cdot$3HCl (previously neutralized with NaOH) to a solution of H-L^B under high dilution conditions in $CHCl_3$ was not successful. The obtained product was an oil containing several compounds that were difficult to be separated. This is not unexpected, as it was already reported that similar self-condensations give rise to differently shaped macrocycles or oligomers.[7,10] Consequently, the template procedures, following routes A, B, C, D or E depicted in Scheme 2, were successfull in the synthesis of mononuclear and f,f$'$ LnLn$'$ or d,f LnM heterodinuclear or f,f Ln_2 homodinuclear complexes.

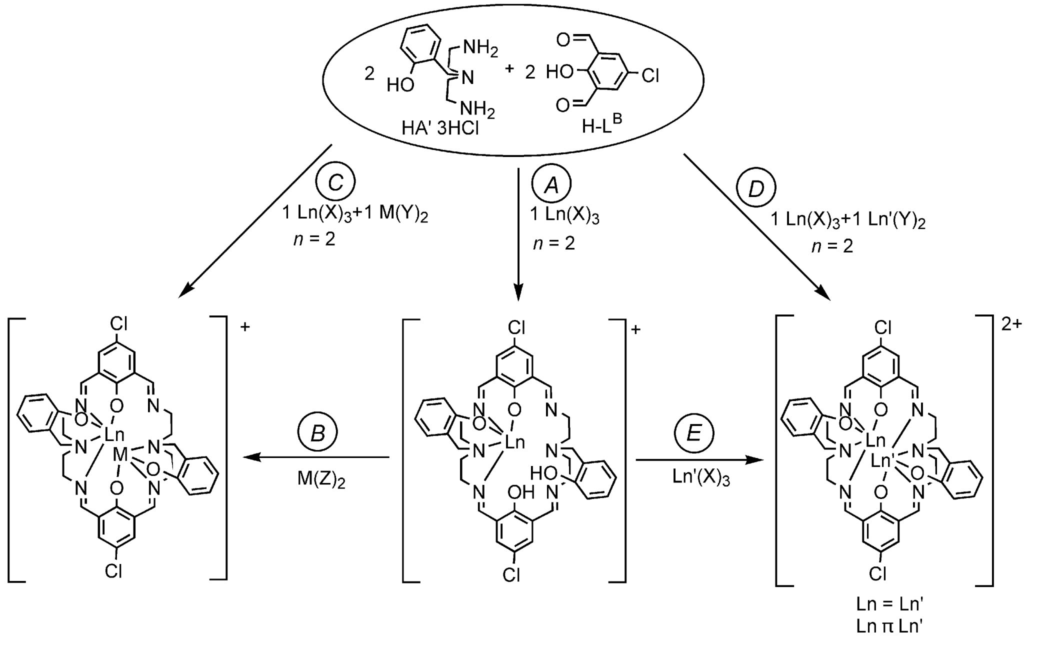

Scheme 2.

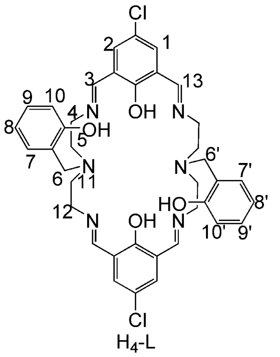

Scheme 3.

Mononuclear Complexes

To avoid acetal formation, experienced in the preparation of the [2+1] acyclic complexes, procedure A (Scheme 2) was successfully tested to obtain the designed macrocyclic species. In particular, the addition of a methanolic solution of HA′·3HCl, $LnX_3 \cdot nH_2O$ (Ln = La, Lu, Y, Gd; X = NO_3^-, CH_3COO^-), and NaOH (stoichiometrically added to neutralize the amine precursor) to a warm $CHCl_3$ solution of H-L^B, followed by the addition of two equivalents of NaOH to favor the deprotonation of two phenolic groups, affords the related mononuclear complexes $[Ln(H_2\text{-}L)(X)] \cdot n$S, as indicated by elemental analysis, ESEM-EDS, and IR spectroscopy. The large excess of chloroform with respect to methanol (95:5) favors the solubility of all the reagents and depresses the formation of acetal groups. The 1:2 H_4-L/NaOH molar ratio in these complexation reactions causes partial deprotonation of the ligand, which according to the experimental data, coordinates the lanthanide(III) ion as the partially deprotonated form $[H_2\text{-}L]^{2-}$ and not in the entirely deprotonated one $[L]^{4-}$. The nitrate and acetate salts were used instead of the chloride salts to avoid the presence of Cl^- as a counteranion in the final complex and to facilitate the ESEM-EDS evaluation of the Ln/Cl ratio and hence of the Ln/$[H_2\text{-}L]^{2-}$ ratio. The formulation of the lanthanum(III) complex as $[La(H_2\text{-}L)(NO_3)] \cdot 0.5CH_2Cl_2$, proposed on the basis of elemental analysis, was supported also by ESEM-EDS measurements, which indicate a La/Cl ratio of 1:3, and was confirmed by ^{1}H and 2D NMR spectroscopic experiments, which show two iminic protons at 8.40 (13-H, 13′-H) and 8.14 ppm (3-H, 3′-H) and the aromatic protons of the diformyl precursors as one broad singlet at 7.62 ppm (2-H, 2′-H), scalar coupled with a doublet at 7.48 ppm (1-H, 1′-H), indicating that one of the two coordinating sites is not involved in coordination.

The yttrium(III) complex $[Y(H_2\text{-}L)(NO_3)] \cdot 3H_2O$ shows a quite simple ^{1}H NMR spectrum in CD_3OD with some small signal shifts from those of the lanthanum(III) analogue. The four iminic protons generate one broad singlet at 8.60 ppm (13-H, 13′-H) and one sharp singlet at 8.32 ppm (3-H, 3′-H). The signals of the aromatic protons of the formyl precursor are characterized by a doublet at 7.76 ppm (2-H, 2′-H) and by a broad singlet at 7.55 ppm (1-H, 1′-H). The peaks of the pendant arms are partially overlapped, but the ^{1}H–^{1}H COSY experiment clarified the spectrum. The aliphatic region presents a series of multiplets attributable to geminal couplings due to the asymmetry of the system. Elemental analysis is consistent with the proposed formulation, and the ESEM-EDS analyses indicate a Y/Cl ratio of 1:2. The IR spectra is characterized by one ν(C=N) band at 1658 cm^{-1} (noncoordinated) and one ν(C=N) band at 1638 cm^{-1} (coordinated); the presence of the coordinated nitrate group is confirmed by the bands at 1442 and 1343 cm^{-1}. This mononuclear complex was investigated also by ESI-MS spectrometry in methanol: the parent peak at m/z = 800.83 belongs to the ion $[Y(H_2\text{-}L)]^+$ species.

The same reaction using 2,6-diformyl-4-methylphenol as the diformyl precursor resulted in the analogous complex $[Y(H_2\text{-}L'')(NO_3)]$ as testified by elemental analyses, ESI mass spectrometry, ESEM-EDS, and NMR and IR spectroscopy. In the ^1H NMR spectrum in CD_3OD the signals in the aliphatic region and the signals due to the two pendant arms are superimposable with those of the analogous complex $[Y(H_2\text{-}L)(NO_3)]$, whereas the signals of the imine protons and the protons of the diformyl precursor are shifted upfield. The methyl groups of the aromatic rings generate a singlet at 2.28 ppm. In the ESI mass spectrum the parent peak is at m/z = 761, which corresponds to the $[Y(H_2\text{-}L'')]^+$ fragment, but a small percentage of the species $[Y(H_2\text{-}L'')(NO_3)] + H^+$ at m/z = 823.92 is present.

$[Y(H_2\text{-}L)(NO_3)]\cdot3H_2O$, $[Lu(H_2\text{-}L)(NO_3)]\cdot2H_2O$, and $[La(H_2\text{-}L)(NO_3)]\cdot0.5CH_2Cl_2$ revealed to be suitable starting products for obtaining d,f or f,f′ heterodinuclear complexes through synthetic pathways B and E (Scheme 2).

d,f Heterodinuclear LnM Complexes

The d,f heterodinuclear complexes were obtained by following synthetic routes B and C of Scheme 2. Step-by-step procedure B consists in the reaction of equivalent amounts of the mononuclear lanthanide(III) complex $[Ln(H_2\text{-}L)(NO_3)]\cdot mH_2O$ (Ln = Y, m = 3; Ln = Lu, m = 2) with $Zn(CH_3COO)_2\cdot2H_2O$, $Cd(NO_3)_2\cdot4H_2O$, $Mn(CH_3COO)_2\cdot4H_2O$, or $Ni(CH_3COO)_2\cdot4H_2O$ in methanol to afford the d,f heterodinuclear complexes $[LnM(L)(X)]\cdot xH_2O\cdot yC_2H_5OH$ (X = CH_3COO^-, NO_3^-; x = 2–5; y = 1), whose counteranion is always derived from the incoming metal(II) salt, this indicating a metathesis of the starting complex. In this way, $[ZnY(L)(CH_3COO)]\cdot2H_2O$, $[CdY(L)(NO_3)]\cdot5H_2O$, $[MnY(L)(CH_3COO)]\cdot3H_2O$, $[NiY(L)(NO_3)]\cdot H_2O\cdot C_2H_5OH$, $[ZnLu(L)(CH_3COO)]\cdot3.5H_2O$, and $[LuNi(L)(CH_3COO)]\cdot5H_2O$ were synthesized.

In $[MnY(L)(CH_3COO)]\cdot3H_2O$, resulting from the reaction of $[Y(H_2\text{-}L)(NO_3)]\cdot3H_2O$ and $Mn(CH_3COO)_2\cdot4H_2O$ in the presence of two equivalents of NaOH, the coordinated nitrate group of the starting complex was substituted by an acetate of the manganese(II) salt; this was confirmed by the lack of bands of the coordinated nitrate at 1442 and 1343 cm^{-1} occurring in the mononuclear yttrium(II) complex and the appearance of a ν(C=O) band at 1653 cm^{-1} assigned to the acetate group, possibly acting as a monodentate ligand. One ν(C=N) band at 1648 cm^{-1} is shifted with respect to the ν(C=N) bands of the starting mononuclear yttrium(III) complex (1658 to 1636 cm^{-1}). ESEM-EDS analyses indicate a Y/Mn/Cl ratio of 1:1:2, in agreement with the proposed formulation. The ESI mass spectrum in methanol shows the molecular peak at m/z = 854.17, corresponding to the $[YMn(L)]^+$ species derived from the loss of the acetate counteranion. This indicates a considerable stability of the heterodinuclear core. The subsequent fragmentation of the $[YMn(L)]^+$ species gives rise to two peaks at m/z = 765.78 and m/z = 779.77, assigned to the $\{YMn[(L)\text{-}CH_2C_6H_4OH](OH)\}^+$ and $\{YMn[(L)\text{-}CH_2\text{-}C_6H_4OH + CH_3](OH)\}^+$ species, respectively. Finally, thermal analysis (Figure 1) shows that the YMn complex undergoes weight loss in line with the proposed formulation, giving rise to the mixed oxide $YMnO_3$ whose Y/Mn = 1:1 ratio was determined by ESEM-EDS analyses. The final weight loss at about 1000 °C (79.93 %) agrees well with the calculated value (80.10 %) for the formation $YMnO_3$ as the final product.

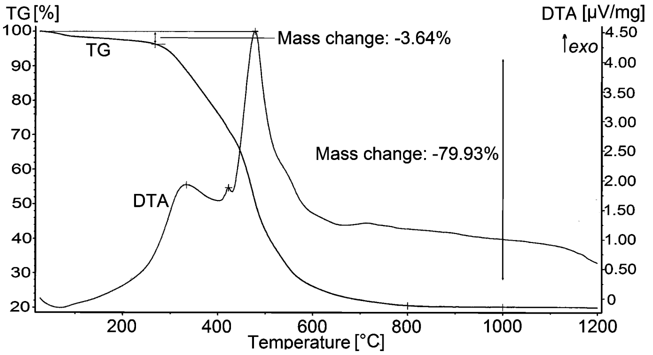

Figure 1. TG-DTA thermogram of $[MnY(L)(CH_3COO)]\cdot3H_2O$.

SEM-EDS analyses of $[LuZn(L)(CH_3COO)]\cdot3.5H_2O$, synthesized from $[Lu(H_2\text{-}L)(NO_3)]\cdot2H_2O$ and $Zn(CH_3COO)_2\cdot2H_2O$, show a Lu/Zn/Cl ratio of 1:1:2, which is consistent with the proposed formulation. In the IR spectrum the nitrate bands, present in the lutetium(III) starting complex, are missing in the LuZn complex, and the ν(C=O) acetate band at 1655 cm^{-1} has been detected. Moreover, the ν(C=N) band of the uncoordinated imine at 1658 cm^{-1} in the mononuclear precursor appears as a strong band at 1648 cm^{-1}, whereas the absorption of the coordinated imine at ca. 1636 cm^{-1} of the mononuclear precursor does not change upon coordination of the transition-metal ion. The peak at m/z = 951.50 corresponding to the $[LuZn(L)]^+$ species in the ESI mass spectrum confirms the stability of the heterodinuclear core.

According to synthetic pathway C (Scheme 2), the template condensation of $H\text{-}L^B$ in $CHCl_3$ with $HA'\cdot3HCl$ in the presence of $Y(NO_3)_3\cdot6H_2O$ or $Lu(NO_3)_3\cdot6H_2O$ and NaOH in CH_3OH followed by the addition of $Zn(CH_3COO)_2\cdot2H_2O$ and NaOH to deprotonate the -OH phenolic groups forms $[YZn(L)(NO_3)]\cdot2CH_3COONa$ and $[LuZn(L)](CH_3COO)\cdot NaCl$ according to SEM-EDS, which ascertains the presence of Na in the correct ratio and elemental analyses. The counteranion of the final complex, derived from synthetic pathway C, is not always that of the incoming transition-metal(II) ion, as the formation of $[YZn(L)(NO_3)]$ shows.

Surprisingly, the success of this synthetic way underlines the stability of the mononuclear lanthanide(III) macrocyclic intermediate that originates from the addition of one equivalent of metal salt and of the equivalents of base necessary for the neutralization of the amine and the deprotonation of two OH phenolic groups. Experimental data, especially the similarity between the LnM complexes obtained by the template and step-by-step procedures, suggest that both synthetic pathways form the mononuclear lanthanide(III) intermediate thanks to the migration of the two remaining protons of the $[H_2\text{-}L]^{2-}$ macrocycle from the phenolic oxygen toward the imine nitrogen atoms, thus preventing the formation of homodinuclear Ln_2 species. The further addition of the transition-metal(II) ion and NaOH, which cause the deprotonation of the other two protons making the phenolic groups prone to act as donor groups for the incoming d metal ion, makes the formation of the heterobimetallic species possible, avoiding the production of a mixture of complexes.

The IR spectra of the LuZn and YZn complexes, obtained by the two different procedures, are superimposable; the only difference is the nitrate stretching bands at 1421 and 1370 cm^{-1} present in the YZn complex obtained with procedure C. In particular, the IR spectra show two strong ν(C=N) bands at ca. 1648 and 1636 cm^{-1}, which corroborate the asymmetry of the obtained d,f complexes. NMR solution studies of d,f complexes obtained by both procedures were not successful because of the high degree of asymmetry arising from complexation. Mass spectrometry was useful in the characterization of the complexes with the identification of the pattern associated with the presence of two different metal ions and two chlorine atoms. In particular, the ESI mass spectrum of $[LuZn(L)](CH_3COO)\cdot NaCl$ is characterized by a peak at $m/z = 951.50$ corresponding to the $[LuZn(L)]^+$ species, whereas $[YZn(L)(NO_3)]\cdot 2CH_3COONa$ is characterized by a peak at $m/z = 865.50$ corresponding to the $[YZn(L)]^+$ species (Figure 2).

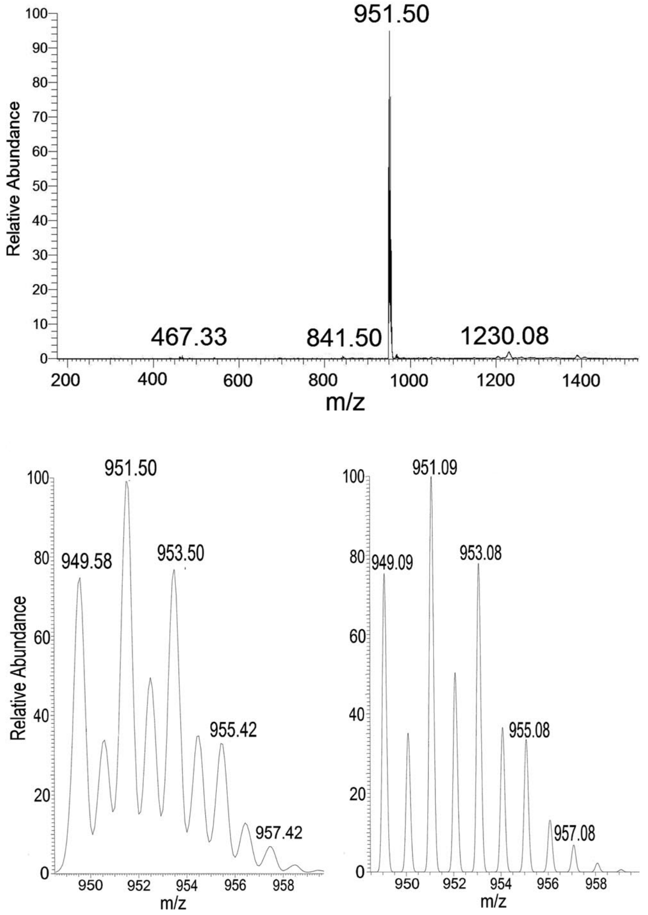

Figure 2. ESI mass spectra of $[LuZn(L)(CH_3COO)]\cdot 3.5H_2O$ (top) with the detailed pattern and MS simulation of the $\{LuZn(L)\}^+$ species (bottom).

Although difficult to interpret, the ^1H NMR spectra in CD_3OD of the YZn and LuZn complexes derived from synthetic route C, parallel each other and parallel the ones of the complexes generated by route B (Scheme 2).

The final products of the thermal decomposition of these complexes, except for the YMn and YNi ones already discussed, contain variable amounts of transition-metal oxides, which under the thermogravimetric conditions are found to be volatile enough to escape from the reaction vessel. The $[LuZn(L)](CH_3COO)\cdot NaCl$ final oxide is composed of, as verified by ESEM-EDS analysis, 80% Lu_2O_3 and 20% ZnO; the weight loss at 1200 °C (81%) agrees with the calculated value (83.6%) for the final product.

f,f Homodinuclear and f,f′ Heterodinuclear Lanthanide(III) Complexes

The f,f′ LnLn′ heterodinuclear and the f,f Ln_2 homodinuclear complexes were prepared by template procedure D or step-by-step procedure E (Scheme 2).

Template procedure D parallels procedure C employed in the synthesis of the d,f heterodinuclear complexes, except for the use of a lanthanide(III) salt instead of a transition-metal(II) one. By this procedure, $[YLu(L)(NO_3)_2]\cdot 5CH_3OH$, $[Lu_2(L)(Cl)_2]\cdot 3.5H_2O$, and $[Y_2(L)(Cl)_2]\cdot 2CH_2Cl_2$ were obtained. For the synthesis of the homodinuclear complexes equivalent amounts of $LnCl_3\cdot nH_2O$, $HA'\cdot 3HCl$, and NaOH in CH_3OH were added to $H\text{-}L^B$ in $CHCl_3$. SEM-EDS analyses of the diyttrium(III) complex reveal a Y/Cl ratio of 2:8 in agreement with the presence of two methylene dichloride solvent molecules. Similarly, in the dilutetium(III) complex, the Lu/Cl ratio of 2:4, found by SEM-EDS analyses, supports the above formulation (Figure 3).

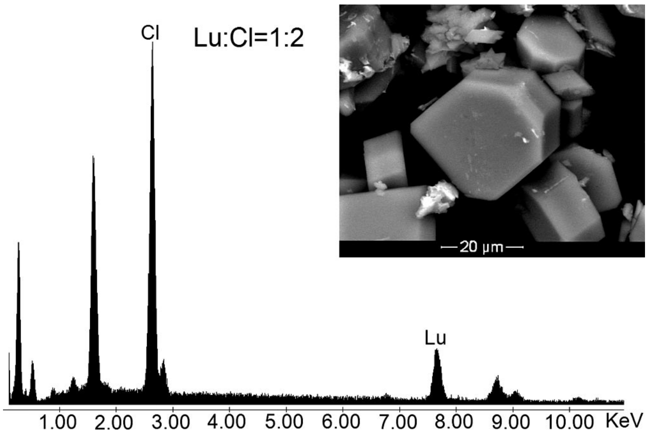

Figure 3. SEM and EDX analyses of the complex $[Lu_2(L)(Cl)_2]\cdot 3.5H_2O$.

Comparison of the IR spectra of the dinuclear complexes with those of the related mononuclear complexes does not show any drastic variations; the ν(C=N) bands at 1657 and 1640 cm^{-1} for the Lu_2 complex and at 1658 and 1639 cm^{-1} for the Y_2 complex are almost similar to those of the mononuclear ones (1658 and 1636 cm^{-1} for the Lu complex and 1658 and 1636 cm^{-1} for the Y one). The very small shifts suggest coordination of the second lanthanide(III) ion remarkably far from the mean plane of the N_3O_2 donor chamber. Furthermore, the presence of two ν(C=N) bands suggests external coordination and the occurrence of an enhanced asymmetry in the homodinuclear complexation. This asymmetry is corroborated also by the ^1H NMR spectra of $[Y_2(L)(Cl)_2]\cdot 2CH_2Cl_2$ in CD_3OD, where the signals of the iminic protons at 8.69 and 8.37 ppm (3-H, 13-H, 3′-H, 13′-H) and of the protons of $[L^A]^-$, represented by two doublets centered at 7.80 and 7.63 ppm (1-H, 2-H, 1′-H, 2′-H), have been detected.

Further evidence of the proposed coordination of the second lanthanide(III) ion comes from the ESI mass spectrum of complex Y_2, which shows one peak at $m/z = 800.92$ corresponding to the mononuclear species $[Y(H\text{-}L) + H]^+$. The ESI mass spectrum of the Lu_2 complex shows one peak at $m/z = 887.25$ corresponding to the mononuclear ion $[Lu(H\text{-}L) + H]^+$.

Although far from the imine groups of $[L]^{4-}$ the lanthanide(III) ion is firmly coordinated, as verified by NMR spectra, probably because of the presence of the pendant arm, which under the ESI-MS conditions easily undergoes protonation and hence releases the metal(III) ion.

The ^1H NMR spectra in CD_3OD of the homodinuclear Y_2 and Lu_2 complexes parallel each other; there are only small shifts and broadening of some signals. The attribution of the signals to the corresponding proton of the ^1H NMR spectra of $[Lu_2(L)(Cl)_2]\cdot 3.5H_2O$ is quite difficult in spite of a very simple ^1H NMR spectrum, this depending on the degree of overlap between the aliphatic signals and the geminal couplings of the protons of the iminic chain. The 2D ^1H–^1H COSY, ^1H–^{13}C HMQC, and ^1H–^1H NOESY experiments, quite useful in the interpretation of the ^1H NMR spectrum, show that the imine protons generate broad and sharp singlets at 8.78 and 8.42 ppm (13-H and 13′-H, 3-H and 3′-H). Furthermore, one doublet at 7.83 ppm and one broad singlet at 7.68 ppm are assigned to the aromatic 2-H, 2′-H and 1-H, 1′-H protons, respectively, according to the coupling between these two signals. The pendant arms with the related aliphatic methylenic 6-H and 6′-H protons are represented by two different sets of peaks properly correlated. The aliphatic region is characterized by two multiplets centered at 3.33 and 3.06 ppm belonging to the geminal 5a–11a-H and 5b–11b-H protons, respectively, whereas the 4-H, 12-H, and 11′-H protons generate one multiplet in the range 4.30–3.99 ppm. The signals of the other protons are split into two multiplets: one in the range 3.18–2.94 ppm and the other hidden by the strong signal of the methanol present in CD_3OD. Finally, the 12′-H and 5′-H protons in the range 3.18–2.94 ppm are coupled with the above cited 11′-H and with 4′-H protons in the range 4.30–3.99 and 3.77–3.52 ppm, respectively (Figures 4 and 5, top).

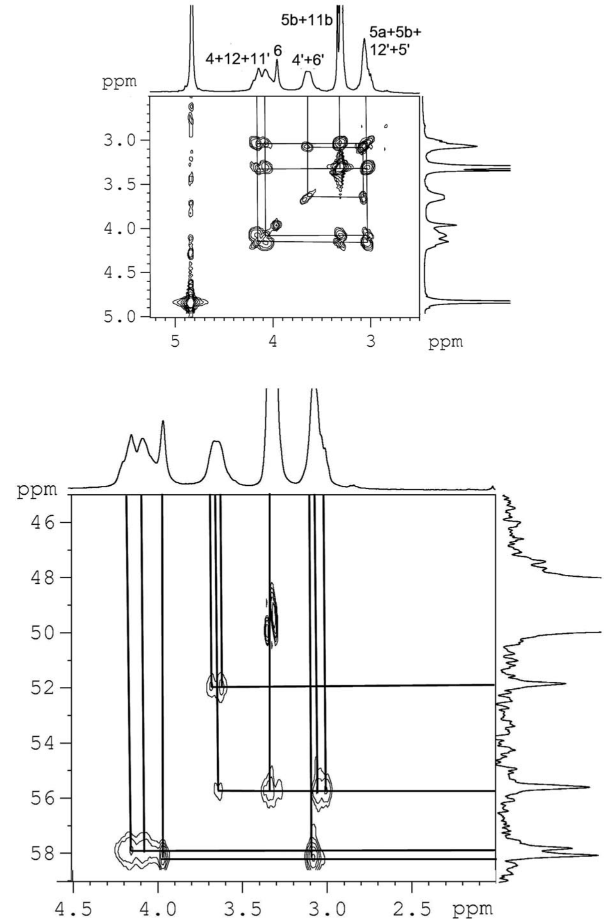

Figure 4. $[Lu_2(L)(Cl)_2]\cdot 3.5H_2O$ in CD_3OD at 298 K: (top) 2D COSY ^1H NMR spectrum; (bottom) 2D HETCORR ^1H–^{13}C HMQC. Geminal correlations in the aliphatic region.

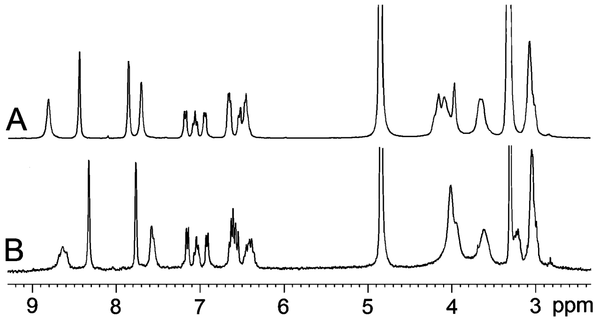

Figure 5. ^1H NMR spectra in CD_3OD at 298 K of (top) $[Lu_2(L)(Cl)_2]\cdot 3.5H_2O$ and (bottom) $[YLu(L)(NO_3)_2]\cdot 5CH_3OH$.

Attempts to recrystallize $[Lu_2(L)(Cl)_2]\cdot 3.5H_2O$ from CH_3OH resulted in separate crystals whose structure corresponds to a dimer of mononuclear $[Lu(L')]_2$ complexes composed of two [2+1] acyclic $[L']^{3-}$ ligands derived from the hydrolysis of the [2+2] cyclic ligand. This indicates that, on standing in alcoholic solution, the dilutetium(III) complex undergoes partial hydrolysis of the imine groups with consequent loss of one lanthanide(III) ion, followed by diacetal formation of the resulting formyl groups and dimerization of the complex to form $[Lu(L')]_2$ (following discussion later).

The heterodinuclear complex $[YLu(L)(NO_3)_2]\cdot 5CH_3OH$ was synthesized according to procedure D (Scheme 2) by the addition of a methanolic solution of *N*,*N*-bis(2-aminoethyl)-2-hydroxybenzylamine·3HCl, $Y(NO_3)_3\cdot nH_2O$, and NaOH (8 equiv.) to a hot $CHCl_3$ solution of H-L^B followed by the addition of $LuCl_3\cdot nH_2O$ and NaOH (2 equiv.). Analogously to procedure C, the first step in procedure D is also represented by the formation of a mononuclear lanthanide(III) complex that consequently evolves into a heterodinuclear complex as a consequence of the addition of the second metal and the remaining amount of base.

SEM-EDS measurements, showing a Y/Lu/Cl ratio of 1:1:2, and elemental analyses agree with the above formulation of the heterodinuclear compound obtained by procedure D. Furthermore, its IR spectrum is quite superimposable on the Y_2 and Lu_2 homodinuclear ones with ν(C=N) bands at 1660 and 1642 cm^{-1}; the only difference is the presence of the two $\nu(NO_3)$ bands at 1421 and 1350 cm^{-1}.

Also, the ESI mass spectra corroborate the formation of a true heterodinuclear complex that is not contaminated by the related homodinuclear analogues owing to the presence of a peak at *m*/*z* = 1035.92 attributable to the $[YLu(L)(NO_3)]^+$ ion. Mass fragmentation generates a peak at *m*/*z* = 929.83, which corresponds to the loss of one pendant arm, as was also verified for other compounds.

The ^{1}H NMR spectra of $[YLu(L)(NO_3)_2]\cdot 5CH_3OH$ in CD_3OD (Figure 5B) reveal an asymmetry of the two pendant arms, which generates quite a complicated system of signals resolved with 2D experiments: one pendant group is characterized by two doublets at 6.91 (7′-H) and 6.56 ppm (10′-H) and one multiplet in the range 6.51–6.29 ppm (8′-H + 9′-H). The other pendant arm shows one doublet at 7.15 ppm (7-H), one triplet at 7.05 ppm (9-H) and one multiplet in the range 6.72–6.58 ppm (8-H + 10-H). The iminic protons generate one broad singlet at 8.63 ppm (13-H, 13′-H) and one sharp singlet at 8.34 ppm (3-H, 3′-H), whereas the aromatic 2-H, 2′-H and 1-H, 1′-H protons generate two doublets at 7.76 and 7.56 ppm, respectively. The aliphatic region was resolved with ^{1}H–^{13}C HMQC, which clarified the presence of *only one geminal coupling* with two multiplets centered at 3.22 and 2.99 ppm, belonging to the 5a,5b-H and 11a,11b-H protons, coupled with the multiplet of the 4-H and 12-H protons (4.22–3.96 ppm). The methylenic 6-H and 6′-H protons generate two singlets at 3.94 and 3.61 ppm, respectively. The other aliphatic chain is characterized by two multiplets at 3.79–3.54 and 3.13–2.99 ppm (11′-H, 5′-H and 4′-H, 12′-H).

Procedure E (Scheme 2) parallels step-by-step procedure B: the addition of one equivalent of $Ln(NO_3)_3\cdot 6H_2O$ and two equivalents of NaOH to $[Y(H_2\text{-}L)(NO_3)]\cdot 3H_2O$, $[Lu(H_2\text{-}L)(NO_3)]\cdot 2H_2O$, or $[La(H_2\text{-}L)(NO_3)]\cdot 0.5CH_2Cl_2$ in CH_3OH affords $[LuY(L)(NO_3)_2]\cdot NaNO_3\cdot CHCl_3$, $[YLa(L)(NO_3)_2]\cdot CH_3OH$, $[LuEr(L)(NO_3)_2]$, $[YEr(L)(NO_3)_2]\cdot 3H_2O$, or $[YLu(L)(NO_3)_2]\cdot H_2O$, whose formulations have primarily been inferred by ESEM-EDS and elemental analyses.

The IR spectra of $[LuY(L)(NO_3)_2]\cdot NaNO_3\cdot CHCl_3$ and $[YLu(L)(NO_3)_2]\cdot H_2O$ obtained from the mononuclear lutetium(III) and yttrium(III) complex, respectively, are almost identical with the same ν(C=N) bands at 1648 and 1640 cm^{-1} and the $\nu(NO_3)$ bands at ca. 1440 and 1345 cm^{-1}; they reveal interesting shifts with respect to the related mononuclear complexes with two ν(C=N) bands at 1658 and 1636 cm^{-1}. The marked differences as regards the YLu and LuY heterodinuclear species derived from template procedure D suggest a stronger contribution of the imine groups in the coordination.

The ^{1}H NMR spectra in CD_3OD of the two YLu complexes are superimposable with that of the complex deriving from procedure D. All these data indicate the equivalence of the two procedures in the formation of heterodinuclear species.

The ESI mass spectra of $[YLu(L)(NO_3)_2]\cdot H_2O$ derived from the mononuclear yttrium(III) complex show two predominant peaks at *m*/*z* = 949.92 and *m*/*z* = 863.92 assigned to the $\{[Lu(H_2\text{-}L)(NO_3)] + H^+\}$ and $\{[Y(H_2\text{-}L)(NO_3)] + H^+\}$ species, respectively, which belong to the mononuclear yttrium(III) and lutetium(III) complexes with nitrate as counteranion. The MS^2 fragmentation of the $\{[Lu(H_2\text{-}L + H)(NO_3)] + H^+\}$ species at *m*/*z* = 949.92 gives rise to one fragment at *m*/*z* = 843.83, corresponding to the mononuclear lutetium(III) complex $\{[Lu(L\text{-}CH_2C_6H_4OH + H)(NO_3)] + H^+\}$ where a pendant arm is substituted by a hydrogen atom. The MS^2 fragmentation of the$\{[Y(H_2\text{-}L)(NO_3)] + H^+\}$ species at *m*/*z* = 863.92 gives rise to one fragment at *m*/*z* = 757.92, corresponding to the mononuclear yttrium(III) complex $\{[Y(L\text{-}CH_2C_6H_4OH + H)(NO_3)] + H^+\}$ where a pendant arm is substituted by a hydrogen atom.

The ESI mass spectra of $[LuY(L)(NO_3)_2]\cdot NaNO_3\cdot CHCl_3$ derived from the mononuclear and lutetium(III) complex show one peak at *m*/*z* = 1036.08 corresponding to the $\{LuY(L)(NO_3)\}^+$ species. The MS^2 fragmentation generates one peak at *m*/*z* = 929.83 attributed to the $\{LuY(L\text{-}CH_2C_6H_4OH + H)(NO_3)\}^+$ species where a pendant arm is substituted by a hydrogen atom.

Unlike the NMR and IR spectroscopic investigations that show that the spectra of the same complexes, prepared by the different routes of Scheme 2, are mainly superimposable, the ESI mass spectra reveal that, under similar experimental conditions, only $[LuY(L)(NO_3)_2]\cdot NaNO_3\cdot CHCl_3$ shows the molecular peak of the $[LuY(L)(NO_3)]^+$ species. This might be due to the different ionic radii of the two lanthanide ions and to the conformation of the macrocycle in consequence of the coordination of the first metal ion, this last fact determining the entire coordination process. In the mononuclear lutetium(III) complex precursor, due to the small radius of the metal ion, the free compartmental chamber is able to better accommodate the larger yttrium(III) ion; on the contrary, in the mononuclear yttrium(III) complex precursor the free compartmental chamber shows greater difficulty in coordinating the incoming lutetium(III) ion. This makes the heterodinuclear complex less stable, at least under the ESI+ MS conditions. Furthermore, the observation that the MS^2 fragmentation of the $[LuY(L)(NO_3)]^+$ species causes the loss of the pendant arm, while the heterodinuclear core still exists, is additional proof that the two metal ions in the LuY complex are strongly linked to the N_3O_2 sites.

By thermal degradation of the YLu complex, the related mixed oxide $YLuO_3$ oxide is obtained, its Y/Lu = 1:1 ratio being inferred by SEM-EDS measurements. The final weight loss at 1100 °C (75.02%) is consistent with the proposed formulation (72.1%). XRD data also agree with those already obtained for mixed oxides derived from thermal degradation of heterodinuclear complexes.[11]

The two yttrium(III) and lutetium(III) mononuclear complexes, when treated with the paramagnetic erbium(III) nitrate salt afford $[LnEr(L)(NO_3)_2]\cdot nH_2O$, according to SEM-EDS analyses, which show a Y/Lu/Er/Cl ration of 1:1:2 and elemental analyses. In the IR spectra of $[YEr(L)(NO_3)_2]\cdot 3H_2O$ the ν(C=N) bands shifted from the values of the mononuclear yttrium(III) complex to 1648 and 1639 cm^{-1} as happens with $[YLu(L)(NO_3)_2]\cdot H_2O$ obtained from the same starting product. The $\nu(NO_3)$ bands are at 1418 and 1365 cm^{-1}. The presence of the erbium(III) ion in these complexes does not allow a detailed NMR investigation, aimed at verifying the influence of the paramagnetic center in the proton signals. Thus, the ^1H NMR spectrum in CD_3OD of the YEr complex shows many hardly attributable peaks in the range from +60 to –40 ppm.

The IR spectra of $[LuEr(L)(NO_3)_2]$ shows two ν(C=N) bands at 1649 and 1638 cm^{-1} analogously to the YEr complex reported above. The ^1H NMR spectrum in $[D_6]DMSO$ of the LuEr complex show 26 signals in the range from 90 to –80 ppm.

Comparison between the ESI mass spectra of the YEr and LuEr complexes reveals an interesting similar behavior with the YLu and LuY complexes obtained from the same starting mononuclear complex. The ESI mass spectra of the YEr complex, as that of the YLu complex, are characterized by the presence of signals with the correct pattern of two mononuclear complexes: $[Y(H\text{-}L) + H]^+$ at m/z = 800.92, with the corresponding Na^+ derivative $[Y(H\text{-}L) + Na]^+$ at m/z = 822.92 and $[Er(H\text{-}L) + H]^+$ at m/z = 879.83 with the corresponding Na^+ derivative $[Er(H\text{-}L) + Na^+]$ at m/z = 901.92. The ESI mass spectra of the LuEr complex, as that of the LuY complex, is characterized by signals of the dinuclear core $[LuEr(L)(NO_3)]^+$ at m/z = 1114.92 whose MS^2 mass fragmentation generates a peak at m/z = 1008.83 corresponding to the loss of one pendant arm $–CH_2\text{-}C_6H_4OH$.

This behavior agrees with the proposal that the ionic radius strongly influences the conformation and hence the stability of the heterodinuclear complex. Again, the loss of the pendant arm, in consequence of the MS^2 fragmentation of the $[LuEr(L)(NO_3)]^+$ ion, clearly shows that the phenol moiety of the pendant arm is not the determining factor in maintaining the heterodinuclear moiety. Unfortunately, attempts to grow suitable crystals to corroborate this proposal structurally failed so far; consequently, we can put forward reasonable proposals that need further X-ray structural confirmation.

X-ray Structure of the $[Lu_2(L')_2]$ Complex

Crystals of $[Lu_2(L')_2]$ were grown from a methanol solution of the crude product. The solid-state structure consists of discrete centrosymmetric dinuclear $[Lu_2(L')_2]$ complexes as shown in Figure 6 (top) with the labeling scheme used.

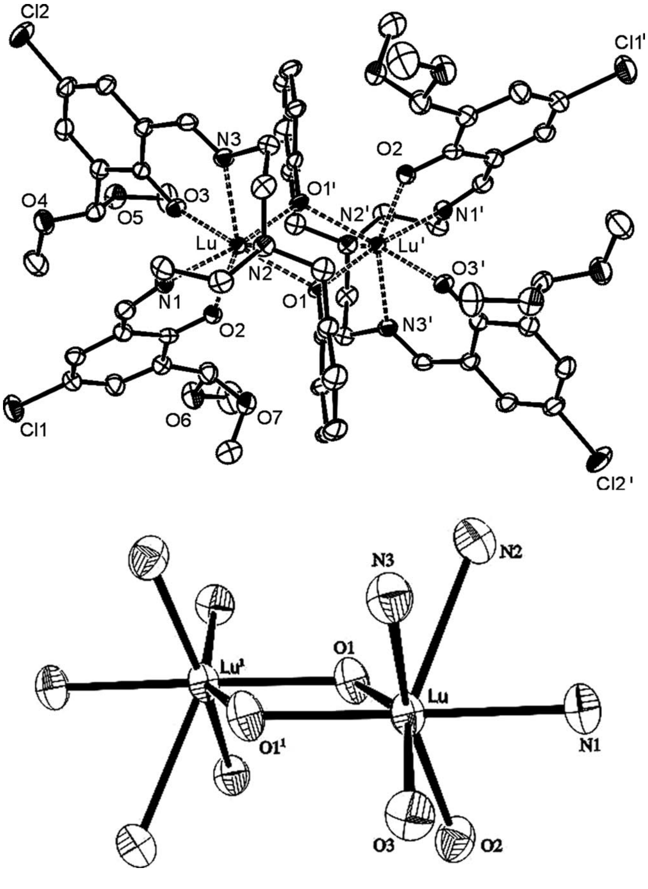

Figure 6. (Top) ORTEP representation of the molecular structure of $[Lu_2(L')_2]$; (bottom) dinuclear Lu^{3+} coordination environment comprised of N and O Schiff base donor atoms.

The hexadentate ligand $[L']^{3-}$ coordinates to the lutetium(III) ion through the two imine and one amine nitrogen atoms (N1, N2, N3), by the two phenoxy oxygen atoms (O2 and O3) and by the bridging O1 oxygen atom of the Schiff base pendant arm. The lutetium(III) ion reaches the seventh coordination by the centrosymmetrically related O1′ atom. The whole system is a centrosymmetric binuclear complex with a Lu_2O_2 rhombic core; the O1···O1′ and Lu···Lu′ contacts are 2.549(4) and 3.700(1) Å, respectively (Figure 6, bottom). The coordination polyhedron around the lutetium(III) ion could be described as a distorted pentagonal bipyramid with N1 and O1′ as apexes (the angle N1–Lu–O1′ is 172.9°). and the base formed by O1, O2, O3, N2, and N3. The distances within the metal ion coordination sphere are: Lu–O1 2.251(3), Lu–N1 2.383(4), Lu–N2 2.660(4), Lu–N3 2.400(4), Lu–O2, 2.167(3), Lu–O3 2.1667(3), and Lu–O1′ 2.242(3) (Table 1), which are comparable to those observed in the dinuclear Schiff base (SB) complex of the general formula $Ln_2(O_2N_2C_{13}H_{20})_3$ (Ln = Nd, Sm, Er)[12] exhibiting seven coordination around the metal ion and in other analogous $Ln(SB)_3$ complexes.[13,14]

Table 1. Selected bond lengths and angles for $[Lu_2L'_2]$.

	Bond lengths [Å]		
Lu–N1	2.383(4)	Lu–N2	2.661(4)
Lu–N3	2.400(4)	Lu–O1	2.251(3)
Lu–O1′	2.242(3)	Lu–O2	2.167(3)
Lu–O3	2.167(3)		
	Bond angles [°]		
O3–Lu–O2	82.4(1)	O3–Lu–O1′	89.8(1)
O2–Lu–O1	83.7(1)	O2–Lu–O1′	83.7(1)
O1–Lu–O1′	69.1(1)	O3–Lu–N1	85.2(1)
O2–Lu–N1	76.2(1)	O3–Lu–N3	74.8(1)
N3–Lu–O1′	84.4(1)	N1–Lu–N3	89.4(2)
O1–Lu–N2	76.4(1)	N1–Lu–N2	68.8(1)
N3–Lu–N2	67.4(1)	O2–Lu–O1′	108.2(1)
O3–Lu–O1	149.6(1)	O1–Lu–N1	117.4(1)
O1–Lu–N1′	172.9(1)	O2–Lu–N3	154.0(1)
O1–Lu–N3	122.2(1)	O3–Lu–N2	133.2(1)
O2–Lu–N2	124.7(1)		

The Lu–O bond lengths of the bridging phenolate [2.251(3) Å] are larger than those of the other coordinated oxygen atoms [2.167(3) Å]. The $Lu–N_{imino}$ distances [2.383(4) and 2.400(4) Å] are shorter than the $Lu–N2_{tertiary}$ distances [2.660(4) Å] and indicate a weak interaction for this latter, related to the requirement of the central atom coordination saturation and to the twisting of the bridging phenolate moieties.

The five membered –Lu–N–C–C–N–diamine chelate ring of the Schiff base adopts the familiar twisted conformation with the torsion angles N1–C11–C12–N2 and N2–C14–C15–N3 of 63.1(5) and 55.2(5)°, respectively.

Conclusions

The symmetric [2+2] macrocycle H_4-L, derived from the condensation of 2,6-diformyl-4-chlorophenol and HA′·3HCl, was used as a suitable ligand for the preparation of f,f homodinuclear and d,f or f,f′ heterodinuclear complexes.

The pendant arm of the amine precursor is the turning point in the possibility to coordinate two large metal ions [i.e., two lanthanide(III) ions] in a relatively small coordinating cavity hosting the second metal ion in a stable, sometimes far from the mean N_3O_3 plane. Different synthetic strategies have successfully been tested. The resulting complexes revealed to be quite useful in the study of the properties arising from metal–metal interactions and in mixed oxide formation. Furthermore, the obtainment of stable mononuclear lanthanide(III) complexes opens new interesting possibilities for specific recognition processes at the free N_3O_3 chamber, which can be engaged in subsequent metal complexation; thus, these systems can act as molecular probes or devices and is currently under investigations.

The stability of the mononuclear complexes, as starting or intermediate ligands in the step-by-step and template reactions, makes the synthesis of pure heterodinuclear LnLn′ or LnM complexes successful, avoiding transmetalation reactions encountered with other dinucleating systems. The d,f complexes resulting from the template or step-by-step reaction revealed to be stable under ESI-MS conditions without fragmentation of the dinuclear core. Furthermore, the formation of acyclic diformyl complexes is under scrutiny to set up a convenient synthetic route for the synthesis of asymmetric macrocyclic complexes.

Experimental Section

Materials: All the salts and solvents were commercial products used without further purification. The diformyl precursor 2,6-diformyl-4-chlorophenol (H-L^B) was prepared according to literature[15] by MnO_2 oxidation of the related 2,6-dimethyl-4-chlorophenol in $CHCl_3$ and purified by chromatography on silica gel ($CHCl_3$/CH_3OH, 95:5). The diformyl precursor 2,6-diformyl-4-methylphenol (H-L^B) was purchased and used without any further purification. Also, the amine precursor *N*,*N*-bis(2-aminoethyl)-2-hydroxybenzylamine·3HCl (HA′·3HCl) was prepared according to the literature by heating a mixture of diethylenetriamine (1.03 g, 10 mmol) and salicylaldehyde (2.44 g, 20 mmol) in EtOH (200 mL) at reflux for 30 min. After the resulting solution was cooled to room temperature, 2-bromomethylphenyl acetate (2.28 g, 10 mmol) and Na_2CO_3 (1.06 g, 10 mmol) were added, and then the solution was heated at reflux for 36 h. Upon cooling to room temperature, the excess amount of solid Na_2CO_3 was filtered off and the filtrate was concentrated under reduced pressure. Yellow deposits were collected and recrystallized from ethanol. The purity and the proposed formulation of both the precursors were checked by elemental analysis, ESI-MS, and IR and NMR spectroscopic measurements.

Physicochemical Measurements: Elemental analyses were carried out by using a Fison 1108 analyzer. IR spectra were recorded as KBr pellets with a Mattson FTIR spectrometer and as powders with a Nicolet Magna-560 equipped with a Continuum Spectra-Tech microscope. NMR spectra (^{1}H, ^{13}C) were recorded with a Bruker AMX300 spectrometer equipped with direct and inverse broad-band multinuclear probes. The T1 longitudinal relaxation times and the mixing times of NOESY experiments were measured by using the standard inversion recovery pulse sequence. All ESI mass spectrometric measurements were performed by using an ESI-MS spectrometer (ThermoFisher LCQ-Fleet) and methanolic solutions of the samples (10^{-5} to 10^{-6} M). Thermogravimetric (TG) and differential thermoanalyses (DTA) curves were obtained by using a Netzsch STA449 thermoanalyzer equipped with Saft Proteous Netzsch software. The measurements were carried out in the range 35–1200 °C in alumina crucibles in air (flux rate 50 $cm^3 min^{-1}$) and a heating rate of 5 °C min^{-1}, using neutral alumina as reference material.

X-ray Measurements and Structure Determination for $Lu_2(L)_2$: The intensity data were collected at room temperature by using a Philips PW1100 diffractometer by using graphite monochromated Mo-K_α radiation (0.71073 Å), following the standard procedures at room temperature. There were no significant fluctuations in the intensities other than those expected from Poisson statistics. All intensities were corrected for Lorentz polarization and absorption.[16]

The structures were solved by standard direct methods.[17] Refinement was carried out by full-matrix least-squares procedures (based on F_0^2) by using anisotropic temperature factors for all non-hydrogen atoms. Hydrogen atoms were placed in calculated positions with fixed, isotropic thermal parameters (1.2 U_{equiv} of the parent carbon atom). The calculations were performed with the SHELXL-97[18] program implemented in the WinGX package.[19] Crystallographic and experimental details for the structure are summarized in Table 2.

Table 2. Crystal and refinement data for $Lu_2(L')_2$.

Empirical formula	$C_{62}H_{68}Cl_4Lu_2N_6O_{14}$
Formula weight	1612.96
Crystal system	monoclinic
Space group	$P2_1/n$
a [Å]	13.909(3)
b [Å]	15.507(3)
c [Å]	14.86(3)
β [°]	98.86(3)
V [A_3]	3158 (1)
Z	2
$D_{calcd.}$ [$g\,cm^{-3}$]	1.696
μ (Mo-K_α) [mm^{-1}]	3.347
$F(000)$	1608
2θ max [°]	50
No. of measured reflections	5520
No. of observations [$I > 2\sigma(I)$]	5172
Parameters	409
R_1, wR_2	0.0395, 0.0961
Goodness of fit	1.197
Δ (max, min) [$e\,Å^{-3}$]	0.902, –0,929

The morphology, homogeneity and the Ln/Cl or Ln/Ln′/Cl ratio of the complexes were investigated by using a Fei-Esem FEI Quanta 200 FEG instrument, equipped with a field emission gun, operating under high-vacuum conditions at an accelerating voltage variable from 0 to 30 keV, depending on the observation needs. EDX analyses and X-ray mapping (elemental mapping) were obtained by using an EDAX Genesis energy-dispersive X-ray spectrometer at an accelerating voltage of 25 keV.

Synthetic Route A

Preparation of $[Ln(H_2\text{-}L)(NO_3)]\cdot nS$: A methanolic solution of $HA'\cdot 3HCl$ (0.6 mmol), $Ln(NO_3)_3\cdot nH_2O$ (0.3 mmol), and NaOH (1.8 mmol) was slowly added to a warm $CHCl_3$ solution of H-L^A (0.6 mmol). The resulting solution was heated at reflux for 15 min and after a further addition of NaOH (0.6 mmol) was maintained under reflux for 2 h. The mixture was then clarified by filtering when hot and allowed to stand. The resulting precipitate was filtered, washed with methanol, and dried in vacuo. When the precipitate did not form, the solvent was evaporated to dryness, and the residue was treated with CH_2Cl_2. The solid was filtered, washed with the appropriate alcohol, and dried in vacuo.

$[La(H_2\text{-}L)(CH_3COO)]\cdot Et_2O$: IR (KBr): ṽ = 1660 (νC=O acetate), 1640 (νC=N uncoordinated), 1630 (νC=N coordinated) cm^{-1}. $C_{44}H_{51}Cl_2LaN_6O_7$ (985.73): calcd. C 53.61, H 5.22, N 8.53; found C 54.22, H 5.05, N 8.92.

$[La(H_2\text{-}L)(NO_3)]\cdot 0.5CH_2Cl_2$: IR (KBr): ṽ = 1656 (νC=N uncoordinated), 1634 (νC=N coordinated), 1414–1331 (νNO_3) cm^{-1}. $C_{38.5}H_{39}Cl_3LaN_7O_7$: calcd. C 48.32, H 4.11, N 10.24; found C 46.80, H 3.77, N 10.96. ^1H NMR (300 MHz, CD_3OD): δ = 8.40 (s, 2 H, 3-H, 3′-H), 8.14 (s, 2 H, 13-H, 13′-H), 7.62 (br. s, 2 H, 2-H, 2′-H), 7.48 (d, 2 H, 1-H, 1′-H), 7.12 (d, 1 H, 7′-H), 7.02 (d, 1 H, 7-H), 6.97–6.85 (m, 2 H, 8′-H, 9-H), 6.71 (d, 1 H, 10′-H), 6.61 (t, 1 H, 9′-H), 6.47 (t, 1 H, 8-H), 6.28 (d, 1 H, 10-H), 3.99–3.85 (m, 2 H, 4′a-H, 12′a-H), 3.80–3.61 (m, 4 H, 4-H, 12-H), 3.80 (s, 2 H, 6-H), 3.77 (s, 2 H, 6′-H), 3.61–3.47 (m, 2 H, 4′b-H, 12′b-H), 3.21–2.69 (m, 8 H, 5-H, 11-H, 5′a-H, 5′b-H, 11′a-H, 11′b-H) ppm.

$[Y(H_2\text{-}L)(NO_3)]\cdot 3H_2O$: IR: ṽ = 1658 (νC=N uncoordinated), 1636 (νC=N coordinated), 1442–1343 (νNO_3) cm^{-1}. ESI-MS: *m*/*z* = 800.83 $[Y(H_2L)]^+$. $C_{38}H_{44}Cl_2N_7O_{10}Y$ (918.58): calcd. C 49.69, H 4.83, N 10.67; found C 49.60, H 5.11, N 10.33. ^1H NMR (300 MHz, CD_3OD): δ = 8.60 (br. s, 2 H, 13-H, 13′-H), 8.32 (s, 2 H, 3-H, 3′-H), 7.76 (s, 2 H, 2-H, 2′-H), 7.55 (s, 2 H, 1-H, 1′-H), 7.16 (d, 1 H, 7-H), 7.03 (t, 1 H, 9-H), 6.91 (d, 1 H, 7′-H), 6.60 (t, 3 H, 8-H, 10-H, 10′-H), 6.41 (t, 1 H, 9′-H), 6.34 (t, 1 H, 8′-H), 4.21–3.82 (m, 8 H, 4-H, 12-H, 6-H, 11′-H), 3.79–3.44 (m, 4 H, 6′-H, 5′-H), 3.26–3.13 (m, 2 H, 5a-H, 11a-H), 3.13–2.93 (m, 6 H, 5b-H, 11b-H, 4′-H, 12′-H) ppm.

$[Lu(H_2\text{-}L)(NO_3)]\cdot 2H_2O$: IR: ṽ = 1658 (νC=N uncoordinated), 1636 (νC=N coordinated), 1455–1340 (νNO_3) cm^{-1}. ESI-MS: *m*/*z* = 886.92 $[Lu(H_2L)]^+$. $C_{38}H_{42}Cl_2LuN_7O_9$ (986.68): calcd. C 46.26, H 4.29, N 9.94; found C 47.94, H 4.32, N 9.52.

$[Gd(H_2\text{-}L)(NO_3)]\cdot 2H_2O$: IR: ṽ = 1656 (νC=N uncoordinated), 1639 (νC=N coordinated), 1450–1345 (νNO_3) cm^{-1}. $C_{38}H_{42}Cl_2GdN_7O_9$ (968.96): calcd. C 47.11, H 4.37, N 10.12; found C 48.22, H 4.29, N 9.69.

Synthetic Route B

Preparation of $[LnM(L)](X)\cdot nS\cdot mH_2O$: To a hot methanol solution of $[Ln(H_2\text{-}L)(NO_3)]\cdot mH_2O$ (Ln = Y, m = 3; Ln = Lu, m = 2) (0.6 mmol) was added $Zn(CH_3COO)_2\cdot 2H_2O$, $Cd(NO_3)_2\cdot 4H_2O$, $Mn(CH_3COO)_2\cdot 4H_2O$ or $Ni(CH_3COO)_2\cdot 4H_2O$ (0.6 mmol), and NaOH (1.2 mmol). The resulting solution was heated at reflux for 2 h, then allowed to stand. The solvent was evaporated to dryness, and the resulting residue was dissolved in methanol. The clarified solution was evaporated to dryness, and the residue was washed with Et_2O or EtOH, then collected by filtration and dried in vacuo.

$[ZnY(L)(CH_3COO)]\cdot 2H_2O$: Et_2O was used as precipitating solvent. IR: ṽ = 1658 (νC=O acetate), 1648 (νC=N coordinated), 1635 (νC=N coordinated) cm^{-1}. ESI-MS: *m*/*z* = 865.00 $[YZn(L)]^+$. $C_{40}H_{43}Cl_2N_6O_8YZn$ (961.04): calcd. C 50.00, H 4.51, N 8.75; found C 50.41, H 4.60, N 8.53. TG weight loss to final oxide Y_2O_3: calcd. 88.3%; found 85.43%.

$[CdY(L)(NO_3)]\cdot 5H_2O$: Et_2O was used as precipitating solvent. IR: ṽ = 1648 (νC=N coordinated), 1634 (νC=N coordinated), 1448–1342 (νNO_3). ESI-MS: *m*/*z* = 913.00 $[YCd(L)]^+$. $C_{38}H_{46}CdCl_2N_7O_{12}Y$ (1065.06): calcd. C 42.86, H 4.35, N 9.21; found C 44.38, H 4.19, N 8.60. TG weight loss to final oxide Y_2O_3: calcd. 89.4%; found 92.2%.

$[MnY(L)(CH_3COO)]\cdot 3H_2O$: Et_2O was used as precipitating solvent. IR: ṽ = 1653 (νC=O acetate), 1648 (νC=N coordinated), 1636 (νC=N coordinated) cm^{-1}. ESI-MS: *m*/*z* = 854.17 $[YMn(L)]^+$. $C_{40}H_{45}Cl_2MnN_6O_9Y$ (968.60): calcd. C 49.60, H 4.68, N 8.68; found C 50.72, H 4.60, N 8.30. TG weight loss to final oxide $YMnO_3$: calcd. 79.89%; found 79.93%.

$[NiY(L)(NO_3)]\cdot H_2O\cdot EtOH$: EtOH was used as precipitating solvent. IR: ṽ = 1646 (νC=N coordinated), 1634 (νC=N coordinated), 1445–1340 (νNO_3) cm^{-1}. ESI-MS: *m*/*z* = 895.08 $[YNi(L)]^+$. $C_{40}H_{44}Cl_2N_7NiO_9Y$ (985.34): calcd. C 48.76, H 4.50, N 9.95; found C 48.30, H 4.07, N 9.25. TG weight loss to final oxide $YNiO_{2.5}$: calcd. 80.96%; found 81.01%.

$[ZnLu(L)(CH_3COO)]\cdot 3.5H_2O$: Et_2O was used as precipitating solvent. IR: ṽ = 1656 (νC=O acetate), 1648 (νC=N coordinated), 1636 (νC=N coordinated) cm^{-1}. ESI-MS: *m*/*z* = 951.50 $[LuZn(L)]^+$.

$C_{40}H_{46}Cl_2LuN_6O_{9.5}Zn$ (1074.09): calcd. C 44.73, H 4.32, N 7.82; found C 46.91, H 4.40, N 7.81.

$[LuNi(L)](CH_3COO)\cdot 5H_2O$: Et_2O was used as precipitating solvent. IR: ṽ = 1658 (νC=O acetate), 1647 (νC=N coordinated), 1634 (νC=N coordinated) cm^{-1}. ESI-MS: *m/z* = 945.50 $[LuNi(L)]^+$. $C_{40}H_{49}Cl_2LuN_6NiO_{11}$ (1094.44): calcd. C 43.90, H 4.51, N 7.68; found C 46.04, H 4.78, N 7.77. TG weight loss to final oxide $LuNiO_{2.5}$: calcd. 74.98%; found 74.65%.

Synthetic Route C

Preparation of $[LnM(L)(X)]\cdot nNaZ$ (Template): A methanolic solution of $HA'\cdot 3HCl$ (0.6 mmol), $Y(NO_3)_3\cdot xH_2O$ or $Lu(NO_3)_3\cdot yH_2O$ (0.3 mmol), and NaOH (1.8 mmol) was added slowly to a warm chloroform solution of H-L^A (0.6 mmol). To the resulting solution, after heating at reflux for 10 min, was added $Zn(CH_3COO)_2\cdot 2H_2O$ (0.3 mmol) and the remaining NaOH (0.6 mmol), and the mixture was heated at reflux for 2 h, then clarified by filtration. Removal of the solvent under reduced pressure gave a residue, which was washed with methanol, filtered, and dried in vacuo.

$[YZn(L)(NO_3)]\cdot 2CH_3COONa$: IR: ṽ = 1656 (νC=O acetate), 1648 (νC=N coordinated), 1635 (νC=N coordinated), 1450–1345 (νNO_3) cm^{-1}. ESI-MS: *m/z* = 865.50 $[YZn(L)]^+$. $C_{42}H_{42}Cl_2N_7Na_2O_{11}YZn$ (1092.04): calcd. C 46.20, H 3.88, N 8.98; found C 46.31, H 3.59, N 8.15.

$[LuZn(L)(CH_3COO)]\cdot NaCl$: IR: ṽ = 1656 (νC=O acetate), 1648 (νC=N coordinated), 1637 (νC=N coordinated) cm^{-1}. ESI-MS: *m/z* = 951.50 $[LuZn(L)]^+$. $C_{40}H_{39}Cl_3LuN_6NaO_6Zn$ (1069.52): calcd. C 44.92, H 3.68, N 7.86; found C 43.88, H 3.62, N 8.42. TG weight loss to final oxide 80% of Lu_2O_3 and 20% ZnO: calcd. 83.6%; found 81%.

Synthetic Route D

Preparation of $[LnLn'(L)(X)_2]\cdot nS$ (Template, Ln = Ln′ and Ln ≠ Ln′)

Ln ≠ Ln′: A methanolic solution of $HA'\cdot 3HCl$ (0.6 mmol), $Y(NO_3)_3$ (0.3 mmol), and NaOH (1.8 mmol) was added slowly to a hot $CHCl_3$ solution of H-L^B (0.6 mmol). $LuCl_3\cdot 6H_2O$ (0.3 mmol) and NaOH (0.6 mmol) were added to the resulting solution, which was heated at reflux for 2 h, then clarified by filtration. Removal of the solvent afforded a residue, which was treated with MeOH or $CHCl_3$, filtered, again washed with methanol, and dried in vacuo.

Ln = Ln′: A methanolic solution of $HA'\cdot 3HCl$ (0.6 mmol), Ln-$(Cl)_3$ (Ln = Y, Lu; 0.6 mmol), and NaOH (3.0 mmol) was added slowly to a warm $CHCl_3$ solution of H-L^B (0.6 mmol). The solution was heated at reflux for 2 h then allowed to stand. The yellow precipitate, obtained for the yttrium(III) complex by addition of $CHCl_3$ and CH_2Cl_2, was collected by filtration, washed with CH_2Cl_2, and dried in vacuo. The solution containing the lutetium(III) complex was evaporated to dryness, and the yellow crystalline powder obtained was treated with fresh methanol, filtered, washed again with methanol, and dried in vacuo.

$[YLu(L)(NO_3)_2]\cdot 5CH_3OH$: IR: ṽ = 1660 (νC=N coordinated), 1642 (νC=N coordinated), 1658.71 (νC=N coordinated), 1385.61 (νNO_3) cm^{-1}. ESI-MS: *m/z* = 1035.92 $[LuY(L)(NO_3)]^+$. $C_{43}H_{56}Cl_2LuN_8O_{15}Y$ (1259.76): calcd. C 41.00, H 4.48, N 8.90; found C 40.92, H 4.40, N 8.81. ^{1}H NMR (300 MHz, CD_3OD): δ = 8.63 (br. s, 2 H, 13-H, 13′-H), 8.34 (s, 2 H, 3-H, 3′-H), 7.76 (d, 2 H, 2-H, 2′-H), 7.56 (d, 2 H, 1-H, 1′-H), 7.15 (d, 1 H, 7-H), 7.05 (t, 1 H, 9-H), 6.91 (d, 1 H, 7′-H), 6.72–6.58 (m, 2 H, 8-H, 10-H), 6.56 (d, 1 H, 10′-H), 6.51–6.29 (m, 2 H, 8′-H, 9′-H), 4.22–3.96 (m, 4 H, 4-H, 12-H), 3.94 (s, 2 H, 6-H), 3.79–3.54 (m, 4 H, 11′-H, 5′-H), 3.61 (s, 2 H, 6′-H), 3.28–3.13 (m, 2 H, 5a-H, 5b-H), 3.13–2.99 (m, 4 H, 4′-H, 12′-H), 3.02–2.95 (11a-H, 11b-H) ppm.

$[Y_2(L)](Cl)_2\cdot 2CH_2Cl_2$: IR: ṽ = 1658 (νC=N coordinated), 1639 (νC=N coordinated) cm^{-1}. ESI-MS: *m/z* = 800.92 [Y(H-L) + H]$^+$. $C_{40}H_{40}Cl_8N_6O_4Y_2$ (1130.30): calcd. C 42.51, H 3.57, N 7.44; found C 44.10, H 3.36, N 7.53. ^{1}H NMR (300 MHz, CD_3OD): δ = 8.69 (s, 2 H, 13-H, 13′-H), 8.37 (s, 2 H, 3-H, 3′-H), 7.80 (br. s, 2 H, 2-H, 2′-H), 7.63 (br. s, 2 H, 1-H, 1′-H), 7.11 (d, 1 H, 7-H), 7.07–6.90 (m, 2 H, 7′-H, 10-H), 6.68–6.39 (m, 5 H, 8-H, 9-H, 8′-H, 9′-H, 10′-H), 4.22–3.94 (m, 6 H, 12-H, 4-H, 11′-H), 3.90 (s, 2 H, 6-H), 3.76–3.58 (m, 4 H, 6′-H, 4′-H), 3.25–3.18 (m, 2 H, 5a-H, 11a-H), 3.15–3.00 (m, 6 H, 5b-H, 11b-H, 5′-H, 12′-H) ppm.

$[Lu_2(L)](Cl)_2\cdot 3.5H_2O$: IR: ṽ = 1657 (νC=N coordinated), 1640 (νC=N coordinated) cm^{-1}. ESI-MS: *m/z* = 887.25 [Lu(H-L) + H]$^+$. $C_{38}H_{43}Cl_4Lu_2N_6O_{7.5}$ (1094.44): calcd. C 38.18, H 3.63, N 7.03; found C 38.61, H 3.54, N 6.75. ^{1}H NMR (300 MHz, CD_3OD): δ = 8.78 (br. s, 2 H, 13-H, 13′-H), 8.42 (s, 2 H, 3-H, 3′-H), 7.83 (d, 2 H, 2-H, 2′-H), 7.68 (br. s, 2 H, 1-H, 1′-H), 7.16 (d, 1 H, 7-H), 7.05 (t, 1 H, 9-H), 6.93 (d, 1 H, 7′-H), 6.69–6.57 (m, 2 H, 8-H, 10-H), 6.52 (d, 1 H, 10′-H), 6.47–6.37 (m, 2 H, 8′-H, 9′-H), 4.30–3.99 (m, 6 H, 4-H, 12-H, 11′-H), 3.96 (s, 2 H, 6-H), 3.77–3.52 (m, 4 H, 6′-H, 4′-H), 3.33 (m, 2 H, 5a-H, 11a-H), 3.18–2.94 (m, 6 H, 5b-H, 11b-H, 5′-H, 12′-H) ppm.

Synthetic Route E

Preparation of $[LnLn'(L)](X)_2\cdot nS$ (Step by Step): $LnX_3\cdot nH_2O$ (0.6 mmol) and NaOH (1.2 mmol) were added to a hot methanolic solution of the desired mononuclear complex $[Ln(H_2\text{-}\mathbf{L})(NO_3)]\cdot nH_2O$ (Ln = Y, *n* = 3; Ln = Lu, *n* = 2; 0.6 mmol). The resulting solution was heated at reflux for 2 h and then allowed to stand. The residue, derived from the evaporation of the solvent, was treated with methanol, and the residue was discharged by filtration. The solution was evaporated to dryness. The resulting residue was treated with $CHCl_3$ or EtOH. The precipitate was filtered, washed, and dried in vacuo.

$[LuY(L)(NO_3)_2]\cdot NaNO_3\cdot 1.5CHCl_3$: IR: ṽ = 1648 (νC=N), 1640 (νC=N), 1442–1338 (νNO_3) cm^{-1}. ESI-MS: *m/z* = 1036.92 $[LuY(L)(NO_3)]^+$. $C_{39.5}H_{37.5}Cl_{6.5}LuN_9NaO_{13}Y$ (1363.64): calcd. C 34.85, H 2.78, N 9.26; found C 31.47, H 2.73, N 10.05. ^{1}H NMR (300 MHz, CD_3OD): δ = 8.6 (br. s, 2 H, 13-H, 13′-H), 8.32 (s, 2 H, 3-H, 3′-H), 7.76 (d, 2 H, 2-H, 2′-H), 7.56 (d, 2 H, 1-H, 1′-H), 7.17 (d, 1 H, 7-H), 7.05 (t, 1 H, 9-H), 6.89 (d, 1 H, 7′-H), 6.74–6.50 (m, 3 H, 8-H, 10-H, 10′-H), 6.44–6.29 (m, 2 H, 8′-H, 9′-H), 4.26–3.77 (m, 6 H, 4-H, 12-H, 6-H), 3.74–3.44 (m, 6 H, 11′-H, 5′-H, 6′-H), 3.19–2.89 (m, 8 H, 4′-H, 12′-H, 5a-H, 5b-H, 11a-H, 11b-H) ppm. TG weight loss to final oxide $LuYO_3$: calcd. 72.01%; found 75.02%.

$[LaY(L)(NO_3)_2]\cdot CH_3OH$: IR: ṽ = 1648 (νC=N), 1637 (νC=N), 1456–1326 (νNO_3) cm^{-1}. $C_{39}H_{40}Cl_2LaN_8O_{11}Y$ (1095.53): calcd. C 42.76, H 3.68, N 10.23; found C 45.62, H 3.81, N 10.54. ^{1}H NMR (300 MHz, [D$_6$]DMSO): δ = 9.00 (s, 2 H, 13-H, 13′-H), 8.26 (s, 2 H, 3-H, 3′-H), 7.73 (d, 2 H, 2-H, 2′-H), 7.41 (d, 2 H, 1-H, 1′-H), 7.14 (d, 1 H, 7-H), 7.09 (t, 1 H, 9-H), 6.98 (d, 1 H, 7′-H), 6.88 (t, 1 H, 9′-H), 6.76 (d, 1 H, 10-H), 6.71 (t, 1 H, 8-H), 6.34 (t, 1 H, 8′-H), 6.19 (t, 1 H, 10′-H), 3.82 (s, 2 H, 6-H), 3.79–3.45 (m, 10 H, 4-H, 12-H, 4′-H, 12′-H, 6′-H), 3.21–2.98 (m, 2 H, 5′b-H, 11′b-H), 2.98–2.59 (m, 6 H, 5b-H, 11b-H, 5′a-H, 11′a-H, 5a-H, 11a-H) ppm.

$[YLu(L)(NO_3)_2]\cdot H_2O$: IR: ṽ = 1648 (νC=N), 1640 (νC=N), 1450–1330 (υ NO_3) cm^{-1}. ESI-MS: *m/z* = 949.92 $\{[Lu(H_2L)(NO_3)] + H\}^+$, 863.92 $\{[Y(H_2L)(NO_3)] + H\}^+$. $C_{38}H_{38}Cl_2LuN_8O_{11}Y$ (1117.56): calcd. C 40.84, H 3.43, N 10.03; found C 41.06, H 3.17, N 9.77. TG weight loss to final oxide $LuYO_3$: calcd. 72.1 %; found 75 %. ^{1}H NMR (300 MHz, CD_3OD): δ = 8.59 (br. s, 2 H, 13-H, 13′-H), 8.31 (s, 2 H, 3-H, 3′-H), 7.76 (d, 2 H, 2-H, 2′-H), 7.56 (d, 2 H, 1-H, 1′-H), 7.15 (d, 1 H, 7-H), 7.05 (t, 1 H, 9-H), 6.91 (d, 1 H, 7′-H), 6.75–6.52 (m, 3 H, 8-H, 10-H, 10′-H), 6.49–6.29 (m, 2 H, 8′-H, 9′-H), 4.20–3.82 (m, 6 H, 4-H, 12-H, 6-H), 3.73–3.49 (m, 6 H, 11′-H, 5′-H, 6′-H), 3.27–3.14 (m, 2 H, 5a-H, 5b-H), 3.14–2.87 (m, 6 H, 4′-H, 12′-H, 11a-H, 11b-H) ppm.

[YEr(L)(NO$_3$)$_2$]: IR: $\tilde{\nu}$ = 1648 (νC=N), 1639 (νC=N), 1455–1337 (νNO_3) cm^{-1}. ESI-MS: *m/z* = 879.83 [Er(H-L) + H]$^+$, 800.92 [Y(H-L) + H]$^+$. $C_{38}H_{36}Cl_2ErN_8O_{10}Y$ (1091.83): calcd. C 41.81, H 3.32, N 10.26; found C 45.26, H 3.50, N 9.86.

[LuEr(L)(NO$_3$)$_2$]·NaNO$_3$: IR: $\tilde{\nu}$ = 1649 (νC=N), 1638 (νC=N), 1452–1339 (νNO_3) cm^{-1}. ESI-MS: *m/z* = 1114.92 [LuEr(L)(NO$_3$)]$^+$. $C_{38}H_{36}Cl_2ErLuN_9NaO_{13}$ (1262.89): calcd. C 36.14, H 2.87, N 9.98; found C 39.16, H 2.74, N 9.42.

CCDC-755076 contains the supplementary crystallographic data for this paper. These data can be obtained free of charge from The Cambridge Crystallographic Data Centre via www.ccdc.cam.ac.uk/data_request/cif.

Supporting Information (see footnote on the first page of this article): IR spectra, SEM data, and NMR spectra of selected compounds.

Acknowledgments

We thank the Ministero dell'Istruzione, dell'Università e della Ricerca (MIUR), Programmi di ricerca di Rilevante Interesse Nazionale (PRIN) (project code 2007W7M4NF) for financial support.

---

[1] a) P. Guerriero, P. A. Vigato, D. E. Fenton, P. C. Hallier, *Acta Chim. Scand.* **1992**, *46*, 1025; b) P. Zanello, S. Tamburini, P. A. Vigato, G. A. Mazzochin, *Coord. Chem. Rev.* **1987**, *77*, 165; c) P. A. Vigato, S. Tamburini, D. E. Fenton, *Coord. Chem. Rev.* **1990**, *106*, 25; d) D. E. Fenton, P. A. Vigato, *Coord. Chem. Rev.* **1988**, *17*, 89; e) P. Guerriero, S. Tamburini, P. A. Vigato, *Coord. Chem. Rev.* **1995**, *134*, 17.

[2] V. Alexander, *Chem. Rev.* **1995**, *95*, 273.

[3] a) D. E. Fenton, H. Okawa, *Chem. Ber./Recueil* **1997**, *130*, 433; b) S. R. Collinson, D. E. Fenton, *Coord. Chem. Rev.* **1996**, *148*, 19; c) D. E. Fenton, *Pure Appl. Chem.* **1986**, *58*, 1437.

[4] a) V. McKee in *Advanced in Inorganic Chemistry* (Ed.: A. G. Sikes), Academic Press, San Diego, USA, **1993**, vol. 40, p. 323; b) J. Nelson, V. McKee, G. Morgan in *Progress in Inorganic Chemistry* (Ed.: K. D. Karlin), Wiley, New York, USA, **1998**, vol. 47, p. 167.

[5] a) S. Brooker, *Coord. Chem. Rev.* **2001**, *222*, 33; b) S. Brooker, *Eur. J. Inorg. Chem.* **2002**, 2535.

[6] S. Tamburini, P. A. Vigato, *Coord. Chem. Rev.* **2004**, *248*, 1718.

[7] P. A. Vigato, S. Tamburini, L. Bertolo, *Coord. Chem. Rev.* **2007**, *251*, 1311–1492.

[8] a) Q. Zeng, M. Qian, S. Gou, H.-K. Fun, C. Duan, X. You, *Inorg. Chim. Acta* **1999**, *294*, 1; b) M. Qian, S. Gou, S. Chantrapromma, S. Sundara Raj, H.-K. Fun, Q. Zeng, Z. Yu, X. You, *Inorg. Chim. Acta* **2000**, *305*, 83; c) M. Qian, S. Gou, Z. Yu, H. Ju, Y. Xu, X. You, *Inorg. Chim. Acta* **2001**, *317*, 157; d) S. Gou, M. Qian, Z. Yu, C. Duan, X. Sun, W. Huang, *J. Chem. Soc., Dalton Trans.* **2001**, 3232.

[9] S. Tamburini, P. A. Vigato, M. Gatos, L. Bertolo, U. Casellato, *Inorg. Chim. Acta* **2006**, *359*, 183–196.

[10] P. A. Vigato, S. Tamburini, V. Peruzzo, *Coord. Chem. Rev.* Work in preparation.

[11] S. Tamburini, P. AVigato, unpublished results.

[12] S. A. Schuetz, M. A. Erdmann, V. W. Day, J. L. Clark, J. A. Belot, *Inorg. Chim. Acta* **2004**, *357*, 4045–4056.

[13] S. A. Schuetz, V. W. Day, R. D. Sommer, A. L. Rheingold, J. A. Belot, *Inorg. Chem.* **2001**, *40*, 5292–5295.

[14] S. A. Schuetz, V. W. Day, A. L. Rheingold, J. A. Belot, *Dalton Trans.* **2003**, 4303.

[15] a) S. Tamguchi, *Bull. Chem. Soc. Jpn.* **1984**, *152*, 126; b) H. Firouzabadi, Z. Mostafavipoor, *Bull. Chem. Soc. Jpn*. **1983**, *56*, 914.

[16] A. T. C. North, D. C. Philips, F. S. Mathews, *Acta Crystallogr., Sect. A* **1968**, *24*, 351.

[17] M. C. Burla, R. Caliandro, M. Camalli, B. Carrozzini, G. L. Cascarano, L. De Caro, C. Giacovazzo, G. Polidori, R. Spagna, *J. Appl. Crystallogr.* **2005**, *38*, 381.

[18] G. M. Sheldrick, *SHELXL-97, Program for the Refinement of Crystal Structures*, University of Göttingen, Germany, **1997**.

[19] L. J. Farrugia, *J. Appl. Crystallogr.* **1997**, *30*, 565.

Received: December 1, 2009